Influence of whole-body dynamics on 15N PISEMA NMR spectra of membrane proteins: A theoretical analysis

ARTICLE *in* BIOPHYSICAL JOURNAL · MAY 2009

Impact Factor: 3.97 · DOI: 10.1016/j.bpj.2008.12.3950 · Source: PubMed

5 AUTHORS, INCLUDING:

Santiago Esteban-Martín
Barcelona Supercomputing Center
31 PUBLICATIONS **603** CITATIONS
SEE PROFILE

Gustavo Fuertes Vives
European Molecular Biology Laboratory
23 PUBLICATIONS **202** CITATIONS
SEE PROFILE

Jesús Salgado
University of Valencia
95 PUBLICATIONS **1,726** CITATIONS
SEE PROFILE

Influence of Whole-Body Dynamics on ^{15}N PISEMA NMR Spectra of Membrane Proteins: A Theoretical Analysis

Santi Esteban-Martín,[†] Erik Strandberg,[‡] Gustavo Fuertes,[†] Anne S. Ulrich,[‡§] and Jesús Salgado[¶*]

[†]Instituto de Ciencia Molecular, Universidad de Valencia, 46980 Paterna (Valencia), Spain; [‡]Karlsruhe Institute of Technology, Institute for Biological Interfaces, Forschungszentrum Karlsruhe, 76021 Karlsruhe, Germany; [§]Institute of Organic Chemistry, University of Karlsruhe, 76131 Karlsruhe, Germany; and [¶]Departamento de Bioquímica y Biología Molecular, Universidad de Valencia, 46100 Burjassot (Valencia), Spain

ABSTRACT Membrane proteins and peptides exhibit a preferred orientation in the lipid bilayer while fluctuating in an anisotropic manner. Both the orientation and the dynamics have direct functional implications, but motions are usually not accessible, and structural descriptions are generally static. Using simulated data, we analyze systematically the impact of whole-body motions on the peptide orientations calculated from two-dimensional polarization inversion spin exchange at the magic angle (PISEMA) NMR. Fluctuations are found to have a significant effect on the observed spectra. Nevertheless, wheel-like patterns are still preserved, and it is possible to determine the average peptide tilt and azimuthal rotation angles using simple static models for the spectral fitting. For helical peptides undergoing large-amplitude fluctuations, as in the case of transmembrane monomers, improved fits can be achieved using an explicit dynamics model that includes Gaussian distributions of the orientational parameters. This method allows extracting the amplitudes of fluctuations of the tilt and azimuthal rotation angles. The analysis is further demonstrated by generating first a virtual PISEMA spectrum from a molecular dynamics trajectory of the model peptide, WLP23, in a lipid membrane. That way, the dynamics of the system from which the input spectrum originates is completely known at atomic detail and can thus be directly compared with the dynamic output obtained from the fit. We find that fitting our dynamics model to the polar index slant angles wheel gives an accurate description of the amplitude of underlying motions, together with the average peptide orientation.

INTRODUCTION

Under physiological conditions, biological membranes are in a fluid-like state (L_α phase) characterized by the intrinsic orientational order of liquid crystals and high thermal disorder (1,2). The constituent molecules, primarily lipids and polypeptides, are aligned and motionally restricted along the membrane normal, and experience considerable freedom to diffuse within the bilayer plane (3). Thus, in these systems the embedded polypeptides orient themselves in a preferred alignment and fluctuate around this orientation in an anisotropic manner. The allowed motions cover a wide range of timescales, as molecules undergo internal and whole-body fluctuations. For instance, membrane proteins may display rotational diffusion about the membrane normal, off-axis reorientation (wobbling), and lateral diffusion on timescales from nanoseconds to milliseconds (4,5), whereas internal peptide-plane librations take place in the picosecond to nanosecond time regime (6,7).

The orientation of a peptide or protein in the membrane generally has direct functional implications (8–10). For this reason, this structural property has attracted much attention and has been the focus of specifically tailored spectroscopic methods (11–15). In particular, solid-state NMR allows determination of the conformation and orientation of membrane-bound peptides and protein fragments. This technique relies on orientation-dependent NMR interactions, namely chemical shift anisotropies, dipole-dipole interactions, and quadrupolar interactions. Among the variety of NMR methods suitable for studying peptides in membranes, the polarization inversion spin exchange at the magic angle (PISEMA) experiment simultaneously measures the pairwise ^{15}N chemical shifts (CS) and ^{1}H-^{15}N dipolar couplings (DC) of all labeled amide bonds, which are displayed in two-dimensional maps (11,16–18). For regular α-helical and β-sheet structures, the PISEMA spectra form characteristic patterns, named polar index slant angles (PISA) wheels, which can be used to obtain the peptide tilt and azimuthal rotation angles (19). Additionally, ^{2}H quadrupolar splittings and ^{13}C and ^{19}F chemical shifts have been successfully used to determine the orientation of peptides in membranes (8,20–24).

Apart from the usual static structural descriptions, the dynamics of membrane-bound peptides have also been investigated. Based on relaxation experiments, motional models were proposed for peptides in membranes, accounting for axial diffusion (10^{-8}–10^{-7} s) and off-axis reorientation fluctuations (10^{-6}–10^{-5} s) (4,5). These motions have important implications for the interpretation of the NMR data, as fluctuations with correlation times faster than the NMR timescale will lead to a partial averaging of the measured parameters. However, although the influence of dynamics on different types of NMR spectra has been noticed (25–29), most structural NMR studies use static models to calculate the peptide orientation, and peptide dynamics is, at most, treated collectively by introducing an order parameter as a scaling factor

Submitted October 19, 2008, and accepted for publication December 18, 2008.

*Correspondence: jesus.salgado@uv.es

Editor: Marc Baldus.

0006-3495/09/04/3233/9 $2.00

doi: 10.1016/j.bpj.2008.12.3950

(8,20). The impact of dynamics for the interpretation of ^{2}H-NMR data has been previously pointed out, based on the results of molecular dynamics (MD) simulations (30,31). A thorough evaluation of various dynamic models for this type of NMR analysis is described in the accompanying article in this issue (32). Briefly, starting from a static model where no motions are allowed, several models of increasing complexity were introduced to account for peptide dynamics. The results clearly support the previous MD analysis (30), showing that the helix tilt angle of a mobile peptide can only be reliably determined when dynamic effects are taken into account.

The effects of small-amplitude motions in ^{15}N-PISEMA experiments have already been explored by simulating such spectra (25), and it was concluded that internal peptide-plane librations may affect the helical wheel patterns. This latter work considers only small internal wobble and librational fluctuations, compared with the much larger amplitudes shown by the MD simulations and our dynamic ^{2}H-NMR analysis (30–32). In a more recent investigation, Page et al. describe perturbations on the shape of the PISA wheels of the influenza A M2 proton channel transmembrane domain caused by Gaussian distributions of the tilt and azimuthal rotation angles (28). By considering separately the effects of limited fast rotation about the helix axis or wobbling of the helix, these authors conclude that fluctuations of this type were not present at either sufficiently high frequency or high amplitude to be noticeable in the PISEMA spectra. However, in the reported case, dynamics can be particularly limited by the tetrameric organization of the peptide hydrophilic pore, where the individual helices may be further anchored because of their amphipathic character (29). Thus, to expand this view, we perform here a more general study that shows the expected effects of dynamics on two-dimensional PISEMA spectra for a wide range of peptide fluctuating cases and a full range of realistic orientations.

For rigid peptides (without any internal conformational fluctuations) with a uniform α-helical structure, the PISEMA NMR observables are calculated with the assumption of moderate to broad Gaussian distributions for the tilt and azimuthal rotation angles. We find that such rigid-body dynamics with amplitudes typical of monomeric peptides can significantly affect the simulated PISEMA spectra. Nevertheless, the typical wheel-like patterns are preserved, and when static models are used to fit these data, the average peptide tilt and azimuthal rotation angles can still be extracted with surprisingly high accuracy, in contrast to the case of a similar ^{2}H-NMR analysis (32). Yet, for peptides undergoing vigorous fluctuations, these fits are accompanied by large errors, which can be considerably reduced by taking the dynamic effects into account in the fitting model. This approach thus allows us to extract quantitative information on peptide dynamics from the PISEMA spectra in the form of the amplitude of the underlying fluctuations together with the average peptide orientation. The validity of such fits to an explicit dynamic model is illustrated here for the monomeric peptide WLP23, whose structure and dynamics are first described by MD simulations (30). These trajectories are then used to generate the corresponding PISEMA spectrum, from which the structural and dynamic parameters are independently reextracted with a striking accuracy.

METHODS

Orientation and dynamics parameters

The model used to describe the peptide orientation and dynamics includes a number of adjustable parameters (Fig. 1). The helix orientation is given by the tilt angle (τ) and the azimuthal rotation angle (ρ), and fluctuations of these two angles are simulated by Gaussian distribution functions (28,30,32):

$$F_i = N\mathrm{e}^{(-(i_0-i)^2/2\sigma_i^2)}, \quad (1)$$

where i refers to the orientation angle, either τ or ρ, N is a normalization constant $(1/\sigma_i\sqrt{2\pi})$, i_0 is the mean of the distribution of the considered angle, and σ_i the standard deviation. Theoretical ^{15}N chemical shifts and ^{1}H-^{15}N dipolar couplings are weighted by the probability distribution and integrated to give time-averaged values. The quality of the fits is assessed from the normalized root mean-square deviation (nrmsd) between the experimental and theoretical values:

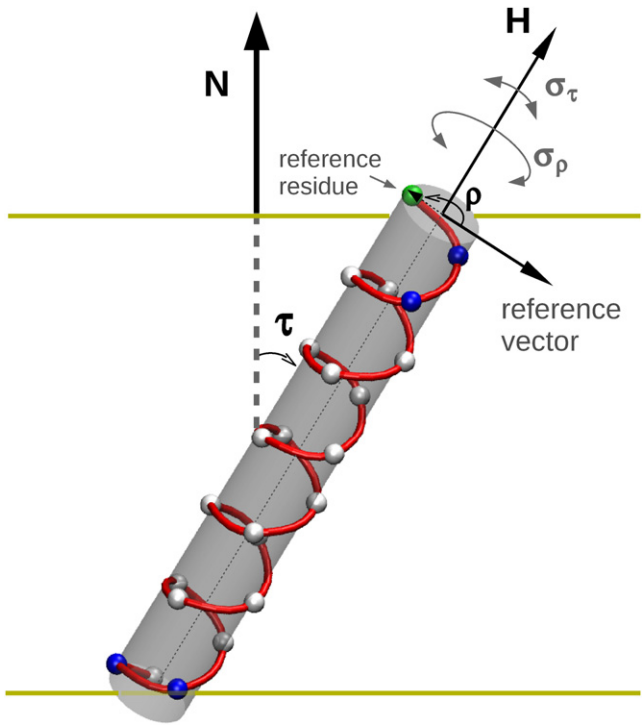

FIGURE 1 Orientational and dynamic parameters for an α-helical peptide in a lipid bilayer. A pair of angles, tilt (τ) and azimuthal rotation (ρ), are sufficient to define the peptide orientation. τ is the angle formed between the molecular long axis of the helix (**H**) and the membrane normal (**N**). We define ρ as the angle between the direction of the peptide tilt and a vector perpendicular to **H**, pointing through the C^α atom of a reference residue (here the first residue of the peptide).

$$\text{nrmsd} = \frac{\text{rmsd}^{\text{CS}}}{\left(\text{CS}^{\text{max}} - \text{CS}^{\text{min}}\right)} + \frac{\text{rmsd}^{\text{DC}}}{\left(\text{DC}^{\text{max}} - \text{DC}^{\text{min}}\right)}, \quad (2)$$

where the normalization factors account for differences in the magnitudes of the dipolar coupling (DC) and chemical shift (CS), and CS^{max}, CS^{min}, and DC^{max}, DC^{min} are the maximum and minimum chemical shifts and dipolar couplings, respectively, measured for each peptide.

An order parameter S, often used to take into account motional averaging from nonspecific molecular fluctuations, is not considered here (equivalent to $S = 1$). Because the effect of this parameter is not fully independent of the tilt and rotational motions, which are included explicitly, if S were used, there would be a wide range of combinations of all dynamics parameters giving very similar results, which increases the uncertainty of the fits (32).

^{15}N chemical shifts and ^{1}H-^{15}N dipolar couplings of ideal α-helices

A two-dimensional PISEMA experiment measures simultaneously the ^{15}N chemical shift and ^{1}H-^{15}N dipolar coupling of each ^{15}N-labeled amide bond, which form a recognizable two-dimensional pattern of resonances (PISA wheel) for regular α-helices. The PISEMA function is given by the following equations:

$$^{15}\text{N CS}_i = \delta_{11}x^2 + \delta_{22}y^2 + \delta_{33}z^2 \quad (3a)$$

$$^{1}\text{H} - ^{15}\text{N DC}_i = \left(b_{\text{NH}}/r_{\text{NH}}^3\right)\left[3\left(\cos\alpha\sin\beta\, x + \sin\alpha\sin\beta\, y + \cos\beta\, z\right)^2 - 1\right], \quad (3b)$$

where x, y, and z are the coordinates of $\mathbf{B}_0$ in the ^{15}N principal axis frame (**PAF**), δ_{11}, δ_{22}, and δ_{33} are the principal values of the chemical shift anisotropy (CSA) tensor ($\delta_{11} \le \delta_{22} \le \delta_{33}$), and α and β are the polar angles by which the dipolar tensor can be rotated into the principal axis frame of the CSA tensor (see Fig. 2). In all cases, we use $\delta_{11} = 56.3$ ppm, $\delta_{22} = 79.0$ ppm, and $\delta_{33} = 224.0$ ppm, which are averages of literature values (25). ^{15}N CSA tensors have been shown to vary from one residue to another in peptides and proteins. However, this variation does not significantly alter the PISA wheels in PISEMA spectra (33). The ^{1}H-^{15}N dipolar coupling constant (b_{NH}) was used as 12,171.5 Hz Å^3, and the length of the N-H bond (r_{NH}) as 1.066 Å, both being averages of experimental NMR data (25). The angle between δ_{33} and the NH bound, which are both assumed to lie in the peptide plane, was taken as $\beta = 16.7^\circ$, and α was set to 0°.

The orientation of the helix axis frame (**HAF**) with respect to $\mathbf{B}_0$ (aligned with the bilayer normal) can be given by the polar coordinates ρ and τ of $\mathbf{B_0}$ in the helix axis frame:

$$\mathbf{B}_0 = \mathbf{HAF}\begin{pmatrix}\cos\rho\sin\tau\\ \sin\rho\sin\tau\\ \cos\tau\end{pmatrix}. \quad (4)$$

The **HAF** and the ^{15}N-**PAF** are related by a matrix **A**, such that **HAF** = **PAF A**, and the coordinates of $\mathbf{B_0}$ in ^{15}N-**PAF** are given by:

$$\begin{pmatrix}x\\ y\\ z\end{pmatrix} = \mathbf{A}\begin{pmatrix}\cos\rho\sin\tau\\ \sin\rho\sin\tau\\ \cos\tau\end{pmatrix}. \quad (5)$$

Then, the associated resonance frequency is computed by substituting Eq. 5 in Eq. 3. The matrix **A** depends on the geometry of the peptide plane and the particular backbone dihedral angles of the helix. Here, we use the model described by Denny (34). Unless stated otherwise, ϕ and ψ backbone dihedral angles are taken as -65° and -40°, respectively.

^{15}N chemical shifts and ^{1}H-^{15}N dipolar couplings from MD simulations

The trajectory of the WLP23 peptide was taken from a previous molecular dynamics simulation, which consists of a set of five replicas amounting to a total of 1 μs simulation time (30). The ^{15}N chemical shifts and ^{1}H-^{15}N dipolar couplings were calculated for each of the 17 core leucines as follows:

$$^{15}\text{N CS}_i = \delta_{11}\sin^2(\theta_i - \beta)\sin^2\lambda_i + \delta_{22}\cos^2\lambda_i + \delta_{33}\cos^2(\theta_i - \beta)\sin^2\lambda_i \quad (6a)$$

$$^{1}\text{H} - ^{15}\text{N DC}_i = \left(b_{\text{NH}}/r_{\text{NH}}^3\right)\left(3\cos^2\theta_i\sin^2\lambda_i - 1\right). \quad (6b)$$

The subscript i denotes each different residue, θ_i is the angle between the amide N-H$_i$ bond and the projection of the magnetic field vector $\mathbf{B}_0$ onto the peptide plane, λ_i is the angle between $\mathbf{B}_0$ and the normal to the peptide plane $\mathbf{N}_i$ (Fig. 2). The molecular interconversion rates between characteristic states of the different replicas studied by molecular dynamics simulations are assumed to be fast compared with the time resolution of the NMR experiment. That way a single time-averaged peak is generated for each virtual labeled residue in the theoretical spectrum.

RESULTS AND DISCUSSIONS

In this dynamic evaluation, we consider two types of motion that can affect the orientation of the peptide molecule: rotational fluctuations about the peptide long axis, which vary the azimuthal angle ρ, and wagging of the helix axis with respect to the membrane normal, which vary the peptide tilt angle τ. Both motions are assumed to be much faster than the characteristic NMR timescales; hence, the calculated chemical shifts and dipolar couplings represent averages over time. These dynamic effects are modeled by means

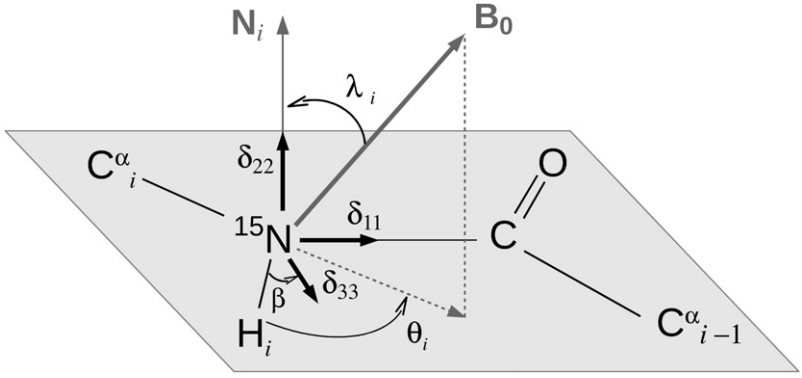

FIGURE 2 Geometry and definition of parameters used to calculate the chemical shift and dipolar splitting for each peptide plane. δ_{11}, δ_{22}, and δ_{33} are the principal components of the CSA tensor, with δ_{22} aligned along the normal to the peptide plane, $\mathbf{N}_i$. The ^{15}N axis frame is related to the ^{1}H-^{15}N dipolar tensor by the angle β. θ_i is the angle between each N-H$_i$ bond and the projection of the magnetic field vector $\mathbf{B}_0$ onto the peptide plane, and λ_i is the angle between $\mathbf{B}_0$ and $\mathbf{N}_i$.

of Gaussian distributions of the respective orientational angles τ and ρ (30,32), each one characterized by a certain mean value (τ_0, ρ_0) of largest probability and a standard deviation (σ_τ, σ_ρ) that represents the amplitude of fluctuations around the preferred value. Because peptides in lipid bilayers are expected to experience both types of motion, distributions of both τ and ρ should be considered simultaneously. Nevertheless, to better understand the contributions of each type, they are also analyzed here separately.

Influence of peptide whole-body motions on PISA wheels

For a typical helical peptide, a PISEMA spectrum directly reflects the helix orientation, particularly its tilt angle. A change in the peptide tilt produces a displacement of the PISA wheel and a change in its size. Thus, in the case of a completely static peptide ($\sigma_\tau = 0°$, *solid lines* in Fig. 3) in a horizontally aligned membrane sample, all signals will lie in the upper-left corner of the PISEMA map when the tilt is small. With an increasing tilt angle the signals migrate toward the bottom of the map, and the wheel size enlarges, which also improves the spectral resolution. At large tilts (approaching 90°) the wheel reduces again in size as it moves toward the right corner of the map.

The consequences of peptide wagging (fluctuation of the helix tilt) are directly related to the above effects. We analyze them by considering a peptide with a fixed azimuthal rotation ρ, undergoing fluctuations of the tilt around an average angle τ_0 with a Gaussian probability distribution σ_τ. The resulting theoretical PISA wheels are shown in Fig. 3 for various mean tilt angles ($\tau_0 = 10°$, 30°, and 90°, panels *A*, *B*, and *C*, respectively) and amplitudes of wagging ($\sigma_\tau = 0°$, 10°, and 20°, within each panel). The tilt distribution reduces the values

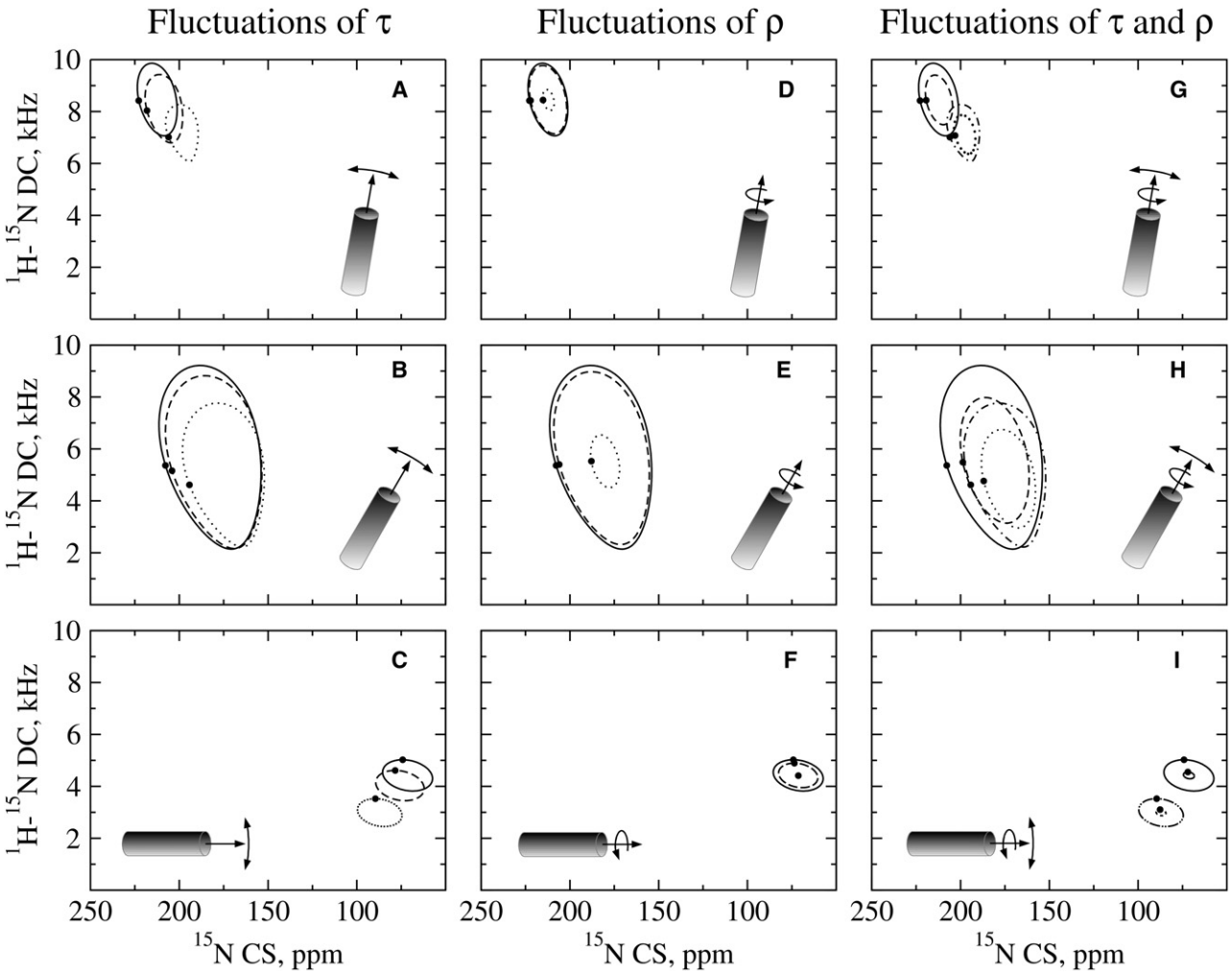

FIGURE 3 PISA wheels corresponding to mean tilt angles of 10° (*A*, *D*, and *G*), 30° (*B*, *E*, and *H*), and 90° (*C*, *F*, and *I*), calculated for various dynamic fluctuation modeled by Gaussian distributions. In each PISA wheel a reference peak is marked with a solid dot, corresponding to a signal from the same residue. Left column (*A–C*): effect of wagging fluctuations of τ, with $\sigma_\tau = 0°$ (*solid line*), 10° (*dashed line*), and 20° (*dotted line*). Middle column (*D–F*): effect of azimuthal fluctuations of ρ, with $\sigma_\rho = 0°$ (*solid line*), 20° (*dashed line*), and 100° (*dotted line*). Right column (*G–I*): effect of simultaneous wagging and azimuthal fluctuations. Shown are σ_τ/σ_ρ pairs of 0°/0° (*solid line*), 0°/50° (*dashed line*), 20°/0° (*dashed-dotted line*), and 20°/50° (*dotted line*).

of the ^{1}H-^{15}N DC and moves the ^{15}N CS toward the isotropic value. This produces a downward displacement and a shrinking of the wheels, compared with the respective static cases, to an extent that is dependent on the value of the mean tilt angle and the amplitude of the fluctuations. Thus, for small and large tilts (Fig. 3, *A* and *C*, respectively), there is a clear displacement of the complete wheel with only a small reduction in the wheel size. However, for intermediate tilts, the displacement affects mainly the signals with larger ^{1}H-^{15}N DC and ^{15}N CS and thereby produces a moderate shift of the wheel center but a distinct change in its size (Fig. 3 *B*). The effects illustrated here for the highest value of $\sigma_\tau = 20^\circ$ are significant and may be chosen to represent the upper limit of fluctuations that can be encountered in membrane-bound peptides (4,5,28,30,32).

Fluctuations of the azimuthal rotation angle about the helix long axis also lead to a partial averaging of the NMR signals. To evaluate specifically the impact of this motion, Gaussian distributions of ρ were analyzed for peptides with a fixed tilt angle. The rotational fluctuations clearly reduce the amplitude of both the DC and CS values. Compared with the effects of wagging, however, this does not shift the position of the PISA wheels, and the dominant effect is a homogeneous reduction in size. Fig. 3 shows examples for tilt angles $\tau_0 = 10^\circ$, 30°, and 90° (panels *D*, *E*, and *F*, respectively), with $\sigma_\rho = 0^\circ$, 20°, and 100° (illustrated in each panel with *solid*, *dashed,* and *dotted lines*, respectively). In the limiting case, when a peptide rotates freely about its own helix axis, the PISA wheels will collapse into a single point, whose position is determined solely by the peptide tilt. It is seen that for $\tau_0 = 90^\circ$, all signals overlap completely already for $\sigma_\rho = 100^\circ$ (Fig. 3 *F*), which corresponds to the upper limit of fluctuations observed for membrane-bound peptides (32).

In a more realistic model of a peptide in a lipid membrane, wagging and rotational fluctuations should be simultaneously present. This case is illustrated by the simulated PISA wheels in Fig. 3, *G–I*, for helices with tilt angles of $\tau_0 = 10^\circ$, 30°, and 90°, respectively. The combined effect of tilt and rotational fluctuations, represented by Gaussian distributions with σ_τ and σ_ρ standard deviations, is consistent with the separate effects of each type of motion. Apart from the direct dependence on the mean tilt angle (τ_0), the position of the wheels is dynamically influenced mainly by σ_τ. The effect is significant for wagging amplitudes that can be encountered with monomeric membrane-bound peptides ($10^\circ < \sigma_\tau < 20^\circ$). In turn, the amplitude of the rotational fluctuations, represented by σ_ρ, principally determines the size of the wheels, affecting signal overlap and spectral resolution, with a different impact depending on the actual tilt of the peptide.

Is the structure analysis affected when dynamics is ignored?

Although it is unrealistic to assume that any peptide in a fluid lipid bilayer has a fixed molecular orientation, NMR studies, particularly PISEMA, typically use static models to calculate the peptide orientation. Because we have seen that PISEMA spectra can be considerably influenced by whole-body motions, the question arises whether the orientational parameters obtained are still accurate when peptide dynamics is neglected in the NMR data analysis. In the accompanying article, it was shown that ^{2}H-NMR analysis can give highly inaccurate results in such cases (32). To address this question now for ^{15}N-PISEMA NMR spectra, we have simulated quasiexperimental PISA wheels as a reference for an ideal peptide with uniform α-helical structure undergoing whole-body motions. These were calculated for the entire range of mean orientations τ_0^{ref} from 0° to 90°, an arbitrarily selected mean value of $\rho_0^{\text{ref}} = 180^\circ$, and several representative standard deviations of σ_τ^{ref} and σ_ρ^{ref}. These virtual spectra of a mobile peptide were then fit to extract the apparent orientational angles using a static model of the same peptide, i.e., purposely ignoring the dynamics. The fits are performed as a grid search over the entire range of 0°–90° and 0°–360° for τ and ρ, respectively. In all cases, we examined a set of ^{15}N CS and ^{1}H-^{15}N DC values for eight (virtual) ^{15}N-labeled residues.

It should be noted that, because we use the same helix conformation and physical parameters to calculate the quasiexperimental spectra and to fit them, in the following analysis the observed drifts can be ascribed exclusively and specifically to the well-defined whole-body dynamics of the peptide, which is explicitly used as an input and is thus being evaluated for several representative cases. If we were to consider real situations, like those studied experimentally, other potential sources of divergence from the models used for the fits would have to be taken into account, such as details of the backbone structure, differences in the individual CSA tensors, and in the relative orientations of the ^{15}N chemical shift and ^{1}H-^{15}N dipolar interaction tensors.

First, we consider the case of our virtual reference peptide undergoing only wagging motions ($\sigma_\rho = 0^\circ$) at different mean tilt values and search for the best fits using a static model. The values of the fitted tilt angles are depicted in Fig. 4, versus the actual tilt of the reference peptide, for different amplitudes of the wagging motions. Up to moderate fluctuations ($\sigma_\tau^{\text{ref}} < 10^\circ$), the fitted peptide tilt angles are very similar to the reference values over the whole range of τ_0^{ref}, with deviations smaller than 10%. Only for strong wagging motions ($\sigma_\tau^{\text{ref}} > 10^\circ$) of helices aligned at tilt angles close to 0° or 90° does the fit produce tilt values that are significantly too large or too small, respectively. This means that, if dynamics is ignored, in cases of helix orientations near 0° and 90°, the tilt angles will be systematically over- or underestimated, respectively. Nevertheless, as we pointed out before, such large wagging fluctuations are not usually expected for membrane-bound peptides.

Next, considering the case where the reference peptide undergoes only rotational fluctuations ($\sigma_\tau = 0^\circ$), we find that the tilt angles obtained by fitting with a static model

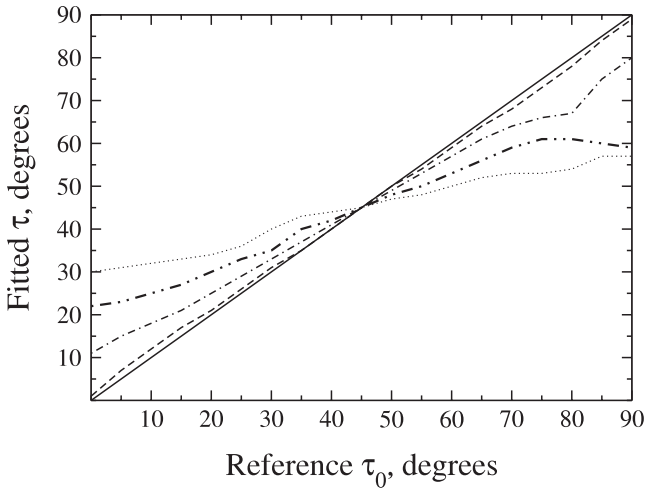

FIGURE 4 Analysis of the deviations encountered on fitting a mobile peptide with a static model. Best-fit τ-values as a function of the actual mean tilt of the reference peptide, which is a virtual case with a rotation angle of 180° undergoing wagging fluctuations with $\sigma_\tau^{ref} = 10°$ (*dashed line*), 20° (*dashed-dotted line*), 30° (*dotted-dashed line*), and 40° (*dotted line*). The solid line corresponds to the perfect fit for $\sigma_\tau^{ref} = 0°$.

are always very close to the reference values (not shown), as anticipated from the simulated spectra in Fig. 3, *D–F*. In all these cases the fitted ρ-values are also very similar to the actual azimuthal rotation angle of the reference peptide, which has been set here arbitrarily at 180°. We have also simulated PISEMA reference spectra for the case of a typical peptide undergoing both wagging and rotational fluctuations for the entire range of τ_0^{ref} from 0° to 90°, using $\rho_0^{ref} = 180°$, $\sigma_\rho^{ref} = 50°$, and $\sigma_\tau^{ref} = 10°$. Fits against these virtual data using a static model produce tilt values that are almost coincident with the actual tilt angles of the reference for the complete range of τ_0^{ref} from 0° to 90°.

We have thus shown that dynamics can have a significant effect on the appearance of PISEMA spectra but that it is still possible to determine the peptide tilt and azimuthal rotation angles rather accurately even if their mobility is ignored in the analysis. This conclusion is in contrast to the situation of calculating tilt angles from ^{2}H-NMR data (32). In line with these observations, the tilt angles determined from ^{2}H-NMR data of several model peptides WLP/WALP and KLP/KALP were systematically smaller than predicted from MD simulations (30,31,35). The reported tilt angles were also smaller than expected for scenarios of positive hydrophobic mismatch (35–39). On the other hand, it was noticed, although from different systems, that the tilt angles of transmembrane peptides determined from ^{15}N-PISEMA data were usually larger than the values from ^{2}H-NMR data and that they had a stronger mismatch dependence (38–41). Our present analysis confirms that PISEMA data, unlike ^{2}H-NMR data (32), can in most cases be safely interpreted without the need to take dynamics into account. This finding is always valid for intermediate tilt angles ~45° and holds for any tilt undergoing only moderate fluctuations ($\sigma_\tau < 10°$, see Fig. 4). Because most peptide helices that have been studied by PISEMA are arranged as oligomers (39,41,42) and are thus expected to exhibit moderate dynamics (28), the previously published results appear to be correct, even though only static models have been used.

Can information on dynamics be extracted from PISEMA data?

Application of a suitable dynamic model in the data analysis can in principle give insights into the amplitudes of fluctuations, as illustrated by the interpretation of ^{2}H-NMR data in the accompanying article (32). In that case we found that the

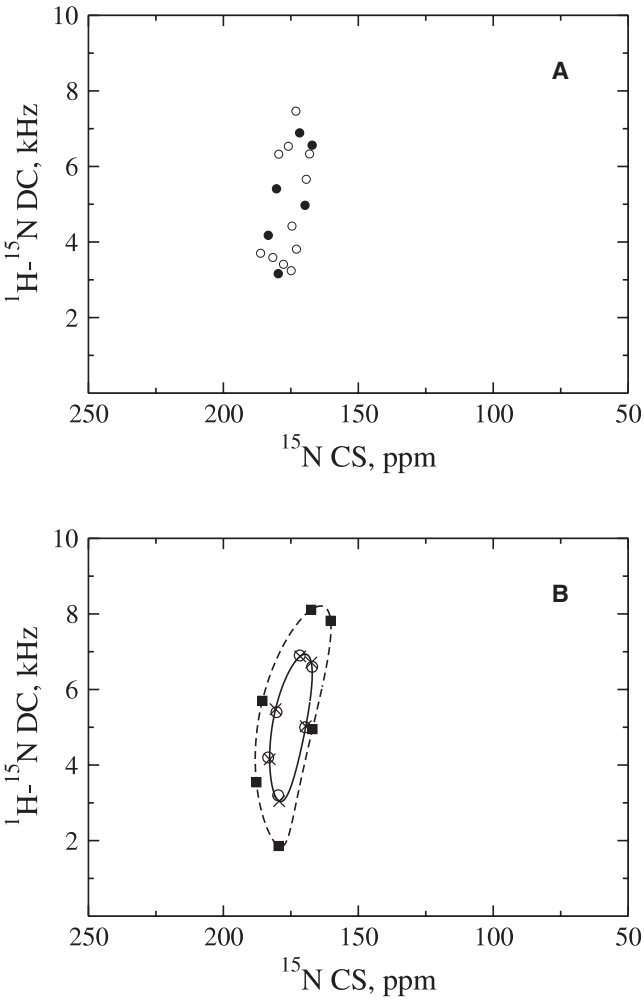

FIGURE 5 Virtual PISEMA spectra of WLP23 in a dimyristoylphosphatidylcholine membrane calculated from the trajectories of an atomistic MD simulation (30). (*A*) All signals corresponding to the 17 leucine residues of the peptide are shown, with those of the six residues used here for the fits (positions 10–15) marked with solid circles. (*B*) Best-fit PISA wheels to the virtual PISEMA spectrum of WLP23. The six quasiexperimental signals of residues 10–15, used here for the fits, are marked with open circles. The dashed line is the best-fit PISA wheel corresponding to a static model, where the positions of the fitted signals are marked with solid squares. The solid line is the best-fit wheel calculated with a dynamic model (explicit fluctuations of τ and ρ), where the fitted signals are marked with crosses.

orientational angles and the fluctuation amplitudes can be estimated, even though different combinations of the four parameters τ_0, ρ_0, σ_τ, and σ_ρ may give fits of similar quality. These families of acceptable values were observed as broad and shallow minima of the rmsd function, which permitted us to find at least some limiting values for the orientational and dynamic parameters.

For the analysis of PISEMA data, the accurate access to the averaged τ-and ρ-values, irrespective of dynamics, means that we can include dynamic parameters in the fitting procedure without introducing any ambiguity in the calculated peptide orientation. Yet, for up to moderate peptide fluctuations, there is little margin to guide the search of these additional parameters because the errors are already very close to the intrinsic experimental errors (see an example in Page et al. (28)). For very mobile peptides, on the other hand, the fitting procedure should be sufficiently sensitive to allow determining such additional dynamic parameters, especially along the ^{15}N CS dimension.

We have found no clear-cut example in the literature of experimental PISEMA data on a highly mobile peptide, probably because most studies were carried out with oligomers. Therefore, we decided to generate quasiexperimental PISEMA data for a vigorously fluctuating monomeric peptide by calculating the virtual spectrum from existing MD simulations of WLP23 in dimyristoylphosphatidylcholine bilayers (30). The MD trajectory consists of five replicas of the simulated system, evolving for a total simulation time of 1 μs. During this time, both the helix tilt and azimuthal rotation angles are seen to sample a wide range of values corresponding to broad amplitude distributions (30). For this and for a similar case it has been reported that these distributions can reproduce and explain, to a good approximation, the experimental ^{2}H-NMR splittings measured with the same peptide and lipid membranes (30,31). Thus, although it is only a simulated case, this system can be considered a realistic example of a highly fluctuating monomeric peptide. Note also that the advantage of generating spectra from an MD trajectory is that the complete dynamic input is known for the analyzed system, and it can thus be directly compared with the dynamic output obtained from the fit with the simplified model of whole-body fluctuations.

The experiment-like PISEMA spectrum calculated for the 17 leucine residues of WLP23 in the MD trajectory is shown in Fig. 5 *A*. According to a previous MD study, peptide-plane librations may distort the PISA wheels and give rise to smeared-out patterns (25). However, our spectrum retains the wheel-like features, resembling experimental PISEMA spectra of α-helical peptides, despite the peptide-plane motions and the nonideality of the conformation throughout the trajectory. This finding shows that in our simulations the use of several replicas, each one run for up to 200 ns, samples peptide-plane librations over a large number of different peptide conformations, which effectively average into a fairly uniform structure. The resulting PISA wheel was fit twice, using either a static or a comprehensive dynamic model, as illustrated in Fig. 5 *B*, and the corresponding best-fit parameters are collected in Table 1. As expected, even for such a peptide undergoing vigorous fluctuations of large amplitude ($\sigma_\tau \approx 15^\circ$, $\sigma_\rho \approx 50^\circ$, see discussion above), the fit using a simple static model gives the correct helix tilt and azimuthal rotation angles (34° and 166° from the fit versus 31° and 173° from the simulation, see Table 1). However, the rmsd errors remain large, especially in the chemical shift dimension, which allows further improvement by fitting to a dynamic model. The fitted PISA wheels including fluctuations of τ and ρ indeed have the effect of reducing the errors significantly, for both the ^{1}H-^{15}N DC and for the ^{15}N CS, to values below their usual experimental error (Fig. 5 *B*, *crosses* and *solid line*). Moreover, although the mean tilt and rotation angles remain very similar to the values obtained from the static fit, the amplitudes of wagging and azimuthal fluctuations are found to fit very well to the values calculated directly from the MD simulation (15° and 46° from the fit versus 12° and 58° from the simulation, see Table 1). Note also that this simulated PISEMA spectrum of WLP23 can be fit correctly (with low errors) only when the whole-body motions are taken into account. This is in contrast to the reported case of fitting to the ^{2}H-NMR splittings that had been back-calculated from the same MD trajectory, for which it was possible to

TABLE 1 Orientational angles and dynamic fluctuations of WLP23 as obtained directly from a set of MD trajectories and from a quasiexperimental PISEMA spectrum calculated from these MD simulations

	Orientational parameters		Dynamics parameters		rmsd	
Model	τ (°)*	ρ (°)*	σ_τ (°)†	σ_ρ (°)†	CS (ppm)	DC (kHz)
MD‡	31 (36)	173 (167)	12 (10)	58 (56)	—	—
Fitted, static	34	166	0	0	4.5	1.9
Fitted, dynamic	32	166	15	46	0.4	0.2

MD trajectories are from Esteban-Martín and Salgado (30). Both a static model and a dynamic fluctuation model were used. The best-fit set of parameters is given, corresponding to the rmsd minimum value of the global scoring function (see Methods).

*Averaged values of the distributions.

†Standard deviations of the distributions.

‡For parameters extracted directly from the MD simulation, two values are given, corresponding to the actual distributions and (between parenthesis) to a Gaussian distributions fitted to the MD histogram.

perform similarly good fits with a static model and with various alternative dynamic models (30).

CONCLUSIONS

It is fundamentally important to consider the dynamics of membrane-bound peptides and proteins, as they not only may be of functional relevance but may also have practical consequences for the interpretation of spectroscopic data. For ^{15}N-PISEMA NMR experiments of helical peptides and protein fragments, rigid-body fluctuations will produce changes in the spectral patterns. We find that the standard analysis of PISEMA data (where motions are usually ignored) correctly yields the mean values of the orientational parameters, although a fit with a dynamic model can give a more comprehensive description of the mobile system. Rotational oscillations about the helix long axis mainly change the size of the PISA wheels, whereas off-axis wagging fluctuations affect mostly the wheel position. These effects are negligible for peptides with low mobility, as in the case of oligomers, but are expected to be important for highly mobile monomers. In the latter case, the main features of their wagging and azimuthal fluctuations can be captured by including Gaussian distribution of the orientational angles in the fitting function. Thus, together with the time-averaged peptide tilt and azimuthal rotation angles, the amplitudes of their respective fluctuations can also be determined. Such information will be important to distinguish peptide monomers from oligomers in their membrane-bound state as well as to compare with results from molecular simulations and ultimately help in envisioning realistic functional models.

The Informatics Service of the University of Valencia (SIUV) is thanked for its support and access to computer clusters. S.E. thanks the Spanish Ministerio de Educación y Ciencia (MEC) for a Formacion de Personal Investigador fellowship and the European Molecular Biology Organization for a short-term fellowship. E.S. and A.U. thank the Deutsche Forschungsgemeinschaft-Center for Functional Nanostructures in Karlsruhe for the NMR infrastructure (E1.2).

This work was supported by a grant from the MEC (BFU200767097), which is financed in part by the European Regional Development Fund (ERDF).

REFERENCES

1. Wiener, M. C., and S. H. White. 1991. Fluid bilayer structure determination by the combined use of x-ray and neutron diffraction. I. Fluid bilayer models and the limits of resolution. *Biophys. J.* 59:162–173.
2. Nagle, J. F., and S. Tristram-Nagle. 2000. Structure of lipid bilayers. *Biochim. Biophys. Acta.* 1469:159–195.
3. Singer, S. J., and G. L. Nicolson. 1972. The fluid mosaic model of the structure of cell membranes. *Science.* 175:720–731.
4. Fares, C., J. Qian, and J. H. Davis. 2005. Magic angle spinning and static oriented sample NMR studies of the relaxation in the rotating frame of membrane peptides. *J. Chem. Phys.* 122:194908.
5. Davis, J. H., M. Auger, and R. S. Hodges. 1995. High resolution ^{1}H nuclear magnetic resonance of a transmembrane peptide. *Biophys. J.* 69:1917–1932.
6. North, C. L., and T. A. Cross. 1995. Correlations between function and dynamics: time scale coincidence for ion translocation and molecular dynamics in the gramicidin channel backbone. *Biochemistry.* 34: 5883–5895.
7. Woolf, T. B., and B. Roux. 1994. Molecular dynamics simulation of the gramicidin channel in a phospholipid bilayer. *Proc. Natl. Acad. Sci. USA.* 91:11631–11635.
8. Glaser, R. W., C. Sachse, U. H. N. Dürr, P. Wadhwani, S. Afonin, et al. 2005. Concentration-dependent realignment of the antimicrobial peptide PGLa in lipid membranes observed by solid-state ^{19}F-NMR. *Biophys. J.* 88:3392–3397.
9. Chen, F., M. Lee, and H. W. Huang. 2003. Evidence for membrane thinning effect as the mechanism for peptide-induced pore formation. *Biophys. J.* 84:3751–3758.
10. García-Sáez, A. J., M. Coraiola, M. Dalla Serra, I. Mingarro, G. Menestrina, et al. 2005. Peptides derived from apoptotic Bax and Bid reproduce the poration activity of the parent full-length proteins. *Biophys. J.* 88:3976–3990.
11. Marassi, F. M., and S. J. Opella. 2000. A solid-state NMR index of helical membrane protein structure and topology. *J. Magn. Reson.* 144:150–155.
12. Jones, D. H., K. R. Barber, E. W. VanDerLoo, and C. W. Grant. 1998. Epidermal growth factor receptor transmembrane domain: ^{2}H NMR implications for orientation and motion in a bilayer environment. *Biochemistry.* 37:16780–16787.
13. Arkin, I. T. 2006. Isotope-edited IR spectroscopy for the study of membrane proteins. *Curr. Opin. Chem. Biol.* 10:394–401.
14. Inbaraj, J. J., T. B. Cardon, M. Laryukhin, S. M. Grosser, and G. A. Lorigan. 2006. Determining the topology of integral membrane peptides using EPR spectroscopy. *J. Am. Chem. Soc.* 128:9549–9554.
15. Nazarov, P. V., R. B. M. Koehorst, W. L. Vos, V. V. Apanasovich, and M. A. Hemminga. 2007. FRET study of membrane proteins: determination of the tilt and orientation of the N-terminal domain of M13 major coat protein. *Biophys. J.* 92:1296–1305.
16. Wu, C. H., A. Ramamoorthy, and S. J. Opella. 1994. High-resolution heteronuclear dipolar solid-state NMR-spectroscopy. *J. Magn. Reson. A.* 109:270–272.
17. Wang, J., J. Denny, C. Tian, S. Kim, Y. Mo, et al. 2000. Imaging membrane protein helical wheels. *J. Magn. Reson.* 144:162–167.
18. Ramamoorthy, A., Y. F. Wei, and D. K. Lee. 2001. PISEMA solid-state NMR spectroscopy. *Ann. R. NMR S.* 52:1–52.
19. Marassi, F. M. 2001. A simple approach to membrane protein secondary structure and topology based on NMR spectroscopy. *Biophys. J.* 80:994–1003.
20. van der Wel, P. C., E. Strandberg, J. A. Killian, and R. E. Koeppe, II. 2002. Geometry and intrinsic tilt of a tryptophan-anchored transmembrane alpha-helix determined by ^{2}H NMR. *Biophys. J.* 83:1479–1488.
21. Toraya, S., K. Nishimura, and A. Naito. 2004. Dynamic structure of vesicle-bound melittin in a variety of lipid chain lengths by solid-state NMR. *Biophys. J.* 87:3323–3335.
22. Salgado, J., S. L. Grage, L. H. Kondejewski, R. S. Hodges, R. N. McElhaney, et al. 2001. Membrane-bound structure and alignment of the antimicrobial beta-sheet peptide gramicidin S derived from angular and distance constraints by solid state ^{19}F-NMR. *J. Biomol. NMR.* 21:191–208.
23. Afonin, S., U. H. N. Dürr, R. W. Glaser, and A. S. Ulrich. 2004. ''Boomerang''-like insertion of a fusogenic peptide in a lipid membrane revealed by solid-state ^{19}F NMR. Magn. *Reson. Chem.* 42:195–203.
24. Strandberg, E., N. Kanithasen, D. Tiltak, J. Bürck, P. Wadhwani, et al. 2008. Solid-state NMR analysis comparing the designer-made antibiotic MSI-103 with its parent peptide PGLa in lipid bilayers. *Biochemistry.* 47:2601–2616.
25. Straus, S. K., W. R. Scott, and A. Watts. 2003. Assessing the effects of time and spatial averaging in ^{15}N chemical shift/^{15}N-^{1}H dipolar correlation solid state NMR experiments. *J. Biomol. NMR.* 26:283–295.

26. Lee, D. K., J. S. Santos, and A. Ramamoorthy. 1999. Application of one-dimensional dipolar shift solid-state NMR spectroscopy to study the backbone conformation of membrane-associated peptides in phospholipid bilayers. *J. Phys. Chem. B*. 103:8383–8390.

27. Dürr, U. H. N., K. Yamamoto, S. Im, L. Waskell, and A. Ramamoorthy. 2007. Solid-state NMR reveals structural and dynamical properties of a membrane-anchored electron-carrier protein, cytochrome b5. *J. Am. Chem. Soc*. 129:6670–6671.

28. Page, R. C., S. Kim, and T. A. Cross. 2008. Transmembrane helix uniformity examined by spectral mapping of torsion angles. *Structure*. 16:787–797.

29. Tian, C., P. F. Gao, L. H. Pinto, R. A. Lamb, and T. A. Cross. 2003. Initial structural and dynamic characterization of the M2 protein transmembrane and amphipathic helices in lipid bilayers. *Protein Sci*. 12:2597–2605.

30. Esteban-Martín, S., and J. Salgado. 2007. The dynamic orientation of membrane-bound peptides: bridging simulations and experiments. *Biophys. J*. 93:4278–4288.

31. Özdirekcan, S., C. Etchebest, J. A. Killian, and P. F. J. Fuchs. 2007. On the orientation of a designed transmembrane peptide: toward the right tilt angle? *J. Am. Chem. Soc*. 129:15174–15181.

32. Strandberg, E., S. Esteban-Martín, J. Salgado, and A. S. Ulrich. 2008. Orientation and dynamics of peptides in membranes calculated from ^{2}H-NMR data. *Biophys. J*. 96:3223–3232.

33. Poon, A., J. Birn, and A. Ramamoorthy. 2004. How does an amide-^{15}N chemical shift tensor vary in peptides? *J. Phys. Chem. B*. 108:16577–16585.

34. Denny, J. K., J. Wang, T. A. Cross, and J. R. Quine. 2001. PISEMA powder patterns and PISA wheels. *J. Magn. Reson*. 152:217–226.

35. Kandasamy, S. K., and R. G. Larson. 2006. Molecular dynamics simulations of model trans-membrane peptides in lipid bilayers: a systematic investigation of hydrophobic mismatch. *Biophys. J*. 90:2326–2343.

36. Mouritsen, O. G., and M. Bloom. 1984. Mattress model of lipid-protein interactions in membranes. *Biophys. J*. 46:141–153.

37. Owicki, J. C., and H. M. McConnell. 1979. Theory of protein-lipid and protein-protein interactions in bilayer membranes. *Proc. Natl. Acad. Sci. USA*. 76:4750–4754.

38. Ramamoorthy, A., S. K. Kandasamy, D. Lee, S. Kidambi, and R. G. Larson. 2007. Structure, topology, and tilt of cell-signaling peptides containing nuclear localization sequences in membrane bilayers determined by solid-state NMR and molecular dynamics simulation studies. *Biochemistry*. 46:965–975.

39. Park, S. H., and S. J. Opella. 2005. Tilt angle of a trans-membrane helix is determined by hydrophobic mismatch. *J. Mol. Biol*. 350:310–318.

40. Song, Z., F. A. Kovacs, J. Wang, J. K. Denny, S. C. Shekar, et al. 2000. Transmembrane domain of M2 protein from influenza A virus studied by solid-state ^{15}N polarization inversion spin exchange at magic angle NMR. *Biophys. J*. 79:767–775.

41. Traaseth, N. J., R. Verardi, K. D. Torgersen, C. B. Karim, D. D. Thomas, et al. 2007. Spectroscopic validation of the pentameric structure of phospholamban. *Proc. Natl. Acad. Sci. USA*. 104: 14676–14681.

42. Duong-Ly, K. C., V. Nanda, W. F. Degrado, and K. P. Howard. 2005. The conformation of the pore region of the M2 proton channel depends on lipid bilayer environment. *Protein Sci*. 14:856–861.